

# Absolute-Magnitude Distributions and Light Curves of Stripped-Envelope Supernovae

Dean Richardson<sup>1,2</sup>, David Branch<sup>1</sup> and E. Baron<sup>1</sup>

## ABSTRACT

The absolute visual magnitudes of three Type IIb, 11 Type Ib and 13 Type Ic supernovae (collectively known as stripped-envelope supernovae) are studied by collecting data on the apparent magnitude, distance, and interstellar extinction of each event. Weighted and unweighted mean absolute magnitudes of the combined sample as well as various subsets of the sample are reported. The limited sample size and the considerable uncertainties, especially those associated with extinction in the host galaxies, prevent firm conclusions regarding differences between the absolute magnitudes of supernovae of Type Ib and Ic, and regarding the existence of separate groups of overluminous and normal-luminosity stripped-envelope supernovae. The spectroscopic characteristics of the events of the sample are considered. Three of the four overluminous events are known to have had unusual spectra. Most but not all of the normal luminosity events had typical spectra.

Light curves of stripped-envelope supernovae are collected and compared. Because SN 1994I in M51 was very well observed it often is regarded as the prototypical Type Ic supernova, but it has the fastest light curve in the sample. Light curves are modeled by means of a simple analytical technique that, combined with a constraint on  $E/M$  from spectroscopy, yields internally consistent values of ejected mass, kinetic energy, and nickel mass.

*Subject headings:* supernovae: individual

## 1. Introduction

In a recent paper (Richardson et al. 2002, hereafter R02) we carried out a comparative study of the absolute magnitudes of all supernovae (SNe) in the Asiago Catalog. Because of the large number of SNe in the sample, we did not attempt to estimate the extinction of each SN in its host galaxy, and we did not assign uncertainties to individual SN absolute magnitudes. In this paper we look more closely at the absolute-magnitude distributions of stripped-envelope supernovae (SE SNe) by assigning uncertainties to each of the quantities that enter into the absolute-magnitude

---

<sup>1</sup>Dept. of Physics and Astronomy, University of Oklahoma, Norman, OK 73019

<sup>2</sup>Physics Dept., Marquette University, Milwaukee, WI 53201

determination, including host galaxy extinction. By SE SNe we mean SNe of Types IIb, Ib and Ic. (The subset containing only SNe Ib and Ic is referred to as SNe Ibc.) The progenitors of SE SNe are stars that have lost most or all of their hydrogen envelopes. This can happen by strong winds such as in Wolf Rayet stars or through mass transfer to a companion star such as in Roche-lobe overflow or a common-envelope phase. The light curves of SE SNe are powered by the radioactive decay of  $^{56}\text{Ni}$ , so the absolute magnitudes are closely related to the ejected  $^{56}\text{Ni}$  masses, and in turn to the stellar progenitors and explosion mechanisms. Since the discovery of the apparent association of GRB980425 with the peculiar Type Ic SN 1998bw (Galama et al. 1999), and the confirmation by spectra of a SN 1998bw-like event associated with GRB030329 (Garnavich et al. 2003), SE SNe have become of intense interest in connection with GRBs. Contamination of high-redshift samples of Type Ia supernovae by SE SNe also is an important issue (Homeier 2005).

We also study the  $V$ -band light curves (LCs) of SE SNe. Data were collected from the literature for two SNe IIb, seven SNe Ib and 11 SNe Ic including three that had unusually broad and blueshifted absorption features in their spectra (we will refer to these as hypernovae). The LCs show considerable diversity in peak brightness, in the width of the peak, and the slope of the late-time tail. In order to relate all of the LCs to total ejected mass, ejected nickel mass, and kinetic energy in an internally consistent way, we fit the data to a simple LC model.

The peak absolute-magnitude data and analysis are described in §2. The light curve data and model fits are presented in §3. A brief summary is given in §4.

## 2. Absolute-Magnitude Distributions

### 2.1. Data

R02 worked with the  $B$  band, but for SE SNe the  $V$  band happens to be the one for which most data are available. In order to calculate the peak visual absolute magnitude for each SN we collected data on the peak apparent visual magnitude, the distance, the foreground Galactic extinction, and the host galaxy extinction, all with assigned uncertainties. We were able to find data for 27 events: three SNe IIb (Table 1), 11 SNe Ib (Table 2) and 13 SNe Ic (Table 3). Eighteen SNe Ibc were in the sample of R02.

#### 2.1.1. Peak Apparent Magnitudes

For most SNe the apparent magnitude and its uncertainty were taken directly from the literature, but in some cases these values were not given so it was necessary for us to estimate them. For SNe 1998dt, 1999di and 1999dn we used an uncalibrated  $R$  band light curve (Matheson et al. 2001) together with a calibrated spectrum to determine the peak  $V$  magnitude. We used the spectrum that was nearest to maximum light to calculate the  $R$  magnitude at that epoch, and used

the  $R$  light curve to determine the  $R$  magnitude at peak. Then we calculated the  $V - R$  color from the spectrum to determine  $V$  at peak. We examined the available data on  $V - R$  versus time for SNe Ibc and estimated the total uncertainty in  $V$  accordingly. A similar method was used for SN 1999cq (Matheson et al. 2000). The peak apparent magnitude for SN 1992ar was taken from Clocchiatti et al. (2000) who, from the limited data available, presented two possible light curves, with different peak magnitudes; we adopted the average. In Tables 1 to 3 we can see that the peak  $V$  magnitudes are the dominant uncertainties in seven cases: the SN IIb 1987K, the SNe Ib 1991D, 1998dt, 1999di and 1999dn, and the SNe Ic 1992ar and 1999cq.

### 2.1.2. Distances

Distance moduli were, for the most part, obtained as in R02. When possible we used a Cepheid calibrated distance to the host galaxy or a galaxy in the same group as the host galaxy. The second choice was the distance given in Tully’s Nearby Galaxies Catalog (Tully 1988), rescaled from  $H_0 = 75 \text{ km s}^{-1} \text{ Mpc}^{-1}$  to our choice of  $H_0 = 60$  for consistency with R02. We adopted an uncertainty of 0.2 magnitudes in the distance modulus, combined in quadrature with the uncertainty resulting from the radial velocity uncertainty of the host galaxy. One significant change since R02 is that a new distance, based on the tip of the red giant branch, has become available for NGC 4214, the host of SN 1954A (Drozdovsky et al. 2002). We adopt this distance in preference to the (longer) Tully distance used in R02. Now SN 1954A no longer appears to be an overluminous SN Ib. Another change is the distance for SN 1994I. This distance is taken from Feldmeier, Ciardullo, & Jacoby (1997) who used the Planetary Nebula Luminosity Function method. In place of the Tully distance to 1990I, we use the distance given by Elmhamdi et al. (2004) which was obtained by the same method. The uncertainty was estimated by considering the difference between the Tully distance and the Elmhamdi distance. The third choice was the luminosity distance (Kantowski, Kao, & Thomas 2000) calculated from the redshift of the host galaxy (in each of these cases  $cz > 2000 \text{ km s}^{-1}$ ) and assuming  $H_0 = 60$ ,  $\Omega_M = 0.3$  and  $\Omega_\Lambda = 0.7$ . A different choice of  $H_0$  would rescale the absolute magnitudes and different choices of  $\Omega_M$  and  $\Omega_\Lambda$  would have very small effects on this sample. The uncertainty in the luminosity distance was calculated assuming a peculiar velocity of  $300 \text{ km s}^{-1}$ . For many of the events of our sample the uncertainty in the distance modulus is significant, although it is dominant only in four cases: SNe 1954A, 1990I, 1997ef and 1998bw.

### 2.1.3. Extinction

The Galactic extinction is from Schlegel, Finkbeiner, & Davis (1998). Values were taken from NED<sup>1</sup> and converted from  $A_B$  to  $A_V$ . In all cases the uncertainties in the Galactic extinction are

---

<sup>1</sup>The NASA/IPAC Extragalactic Database (NED) is operated by the Jet Propulsion Laboratory, California Institute of Technology, under contract with the National Aeronautics and Space Administration.

comparatively small.

When possible the host galaxy extinction and its uncertainty were taken from the literature. When only the equivalent width of the interstellar Na I D lines,  $W(D)$ , in the host was available we calculated  $E(B - V)$  from the relation  $E(B - V) = 0.16W(D)$  (Turatto, Benetti, & Cappellaro 2003) and then used  $A_V = 3.1E(B - V)$ . In this case we took the uncertainty to be as large as the extinction, up to a maximum uncertainty of 1.0 magnitude.

The host galaxy extinction for SN 1983V was taken from Clocchiatti et al. (1997). Porter & Filippenko (1987) reported that the HII region associated with SN 1983V was not as prominent as the one associated with SN 1962L but about the same as the one associated with SN 1964L. Having only this information available we assigned the  $A_V(\text{host})$  value of SN 1983V to SN 1964L. For SN 1962L we took the average value of all other SNe Ic in our sample (which is larger than the extinction of SN 1983V). For SNe 1962L and 1964L we assigned an uncertainty as large as the extinction.

For SN 1990B we took the host galaxy extinction from Clocchiatti et al. (2001). They quoted two values, one determined from the Na I D line and one from the color excess; we chose to use the latter. They did not quote an uncertainty except to say that it was large and unknown, so we assigned a large uncertainty of 1.0 magnitude.

Grothues & Schmidt-Kaler (1991) give the extinction for various regions of NGC 3310, the host galaxy of SN 1991N. Near the position of SN 1991N (Barth et al. 1996) the visual extinction was 1 to 2 magnitudes with an uncertainty of about 1 magnitude. Because the SN was most likely inside rather than behind the H II region this extinction is probably an overestimate. We adopted  $A_V = 1.0 \pm 1.0$ .

SE SNe tend to be associated with star formation so they also tend to be significantly extinguished in their host galaxies. Tables 1 to 3 show that for many events in our sample the uncertainty in the host galaxy extinction is the dominant uncertainty, and overall it is the largest source of absolute-magnitude uncertainty for our sample.

## 2.2. Analysis

Absolute visual magnitude is plotted against distance modulus in Figure 1. The slanted dashed line is the line of constant apparent visual magnitude (less the total extinction) of 16. The horizontal dashed line is the SN Ia “ridge line” at  $M_V = -19.5$ , shown for comparison. The tendency of intrinsically brighter SNe to be at larger distances, and the fact that all but a few of the SNe are to the left of the slanted line, are obvious consequences of the strong observational bias in favor of the discovery and follow-up of brighter SNe. The absence of SNe in the lower right part of the figure is a selection effect against lower-luminosity events at large distance, and the absence of SNe in the upper left is due to the fact that overluminous events are uncommon, so none happen to have been

seen in relatively nearby galaxies. Considering that the events of this sample have been discovered in so many different ways, we make no attempt to correct the absolute magnitude distribution for bias. Instead, we emphasize that in this study we are simply characterizing the available observational sample of SE SNe; a sample in which overluminous events are over-represented relative to less luminous ones.

In Figure 1, there are quite a few SNe Ic in the distance modulus range from about 29 to 32. There are also quite a few SNe Ib in the distance modulus range from 33 to 35. These groups happen purely by chance. There is no spatial connection, other than distance, between the SNe within each of these groups.

R02 considered the possibility that SNe Ibc can be divided into two luminosity groups: normal-luminosity SNe Ibc, and overluminous SNe Ibc that are even more luminous than SNe Ia. We consider that possibility here also. As can be seen in Figure 1, four events of our sample, three SNe Ic and one SN Ib, are above the SN Ia ridge line.

The mean absolute magnitude and its standard deviation, both weighted and unweighted, for the whole sample as well as for several subsets of the sample, are given in Table 4. The weighted mean of the whole sample is  $M_V = -18.03 \pm 0.06$ , with  $\sigma = 0.89$ . When SE SNe are separated into normal-luminosity and overluminous we have  $M_V = -17.77 \pm 0.06$ ,  $\sigma = 0.49$  for the normal-luminosity events and  $M_V = -20.08 \pm 0.18$ ,  $\sigma = 0.46$  for the overluminous. Comparing the normal-luminosity SNe Ib and Ic, the unweighted means differ by 0.54 magnitudes in the sense that SNe Ic are brighter than SNe Ib, but the weighted means differ by only 0.16 magnitudes so a difference between normal-luminosity SNe Ib and Ic is not firmly established by these data.

A histogram of the absolute magnitudes is shown in Fig. 2. Fig. 2 also shows the best Gaussian fit to all of the data, determined by the  $\chi^2$  test using the mean absolute magnitude and dispersion as parameters. The results were  $\bar{M}_V = -18.49$  and  $\sigma = 1.13$ , but the low probability of 15% confirms what is apparent to the eye: the distribution is not adequately fit by a Gaussian.

Considering the possibility of two luminosity groups we also fit the data to a double-peaked distribution. To do this we used:

$$f(x) = f_0 \left( w \exp \left[ -\frac{(x - x_1)^2}{2\sigma_1^2} \right] + \exp \left[ -\frac{(x - x_2)^2}{2\sigma_2^2} \right] \right), \quad (1)$$

with five parameters:  $x_1$  and  $x_2$  (the two mean absolute magnitudes),  $\sigma_1$  and  $\sigma_2$  (the two dispersions) and the weighting factor,  $w$ . The normalization factor,  $f_0$ , is equal to  $(1+w)^{-1}$ . The results for the double-peaked distribution are:  $\bar{M}_{V,1} = -20.31$ ,  $\bar{M}_{V,2} = -18.20$ ,  $\sigma_1 = 0.18$ ,  $\sigma_2 = 0.81$  and  $w = 0.13$ . The probability of this fit is 39%, still quite low.

### 2.3. Comments on Spectra

Here we briefly consider the extent to which SE SNe that have normal luminosities have typical spectra and SE SNe that are overluminous have peculiar spectra.

#### 2.3.1. Type IIb

At early times the spectra of SNe II have conspicuous H $\alpha$  and H $\beta$  P–Cygni features but at later times they resemble the spectra of SNe Ib because the Balmer lines are replaced by He I lines. The early Balmer lines in SN 1996cb are stronger and more similar to those of SN 1987A than to those of SN 1993J (Qiu et al. 1999), which may mean that SN 1996cb had a thicker hydrogen layer than SN 1993J. Overall, however, the spectra of the three SN IIb in the sample are rather similar, and the peak absolute magnitudes are the same within the uncertainties.

#### 2.3.2. Type Ib

Branch et al. (2002) studied the optical spectra of a dozen SNe Ib selected on the basis of having deep He I absorption features. The events of that sample displayed a rather high degree of spectral homogeneity, except that three also contained deep H $\alpha$  absorptions. Of the 11 SNe Ib in the present sample, seven were in the sample of Branch et al. (2002): SNe 1983N, 1984L, 1998dt, 1999dn, 1954A, 1999di, and 2000H, with the last three being the “deep–H $\alpha$ ” events. We find that all seven of these events have absolute magnitudes within the normal SN Ib range, and we see no significant difference between the absolute magnitudes of the deep–H $\alpha$  events and the others.

The single available spectrum (Leibundgut, Phillips, & Graham 1990) of one of the SNe Ib in our present sample, SN 1984I, covers a limited wavelength range so that little can be said except that it does appear to be a SN Ib. Its absolute magnitude is within the normal range.

The spectra of SN 1990I contained typical SN Ib absorption features but they were broader and more blueshifted than those of the Branch et al. (2002) sample (Elmhamdi et al. 2004), although not enough to be considered a hypernova. The absolute magnitude is within the normal range.

SN 1991D has been discussed by Benetti et al. (2002) and Branch (2003). Its He I absorptions were less deep and the velocity at the photosphere near the time of maximum light was lower than in the events of the Branch et al. (2002) sample. Thus the one overluminous SN Ib of our present sample also had an unusual spectrum.

SN 1999ex was observed by Hamuy et al. (2002) who referred to it as an intermediate Type Ib/c because of its relatively weak He I lines. Branch (2003) refers to it as a “shallow helium” SN Ib because its He I lines were clearly present, although weaker than in the events of the Branch et al. (2002) sample. While this event had an unusual spectrum, according to Table 2 its absolute

magnitude is within the normal range.

To summarize SNe Ib: the single overluminous SN Ib of our sample had an unusual spectrum, and most but not all (not SNe 1990I and 1999ex) of the normal-luminosity events had normal spectra.

### 2.3.3. Type Ic

Five events of our sample, SNe 1983I, 1983V, 1987M, 1990B, and 1994I, can be said to have had typical SN Ic spectra. The limited available spectra of three others, SNe 1962L, 1964L, and 1991N, also show no indication of peculiarity. The absolute magnitudes of all eight of these events are within the normal SN Ic range.

As is well known, SN 1998bw was overluminous, and its absorption features were very broad and blueshifted. Two other SNe Ic of our sample, SNe 1997ef (Mazzali, Iwamoto, & Nomoto 2000) and 2002ap (Kinugasa et al. 2002), also had broad spectral features, although not as broad as those of SN 1998bw; these two SNe Ic were *not* overluminous.

Apart from SN 1998bw, the other two overluminous SNe Ic of our sample are SNe 1992ar and 1999cq. Clocchiatti et al. (2000) conclude that the one available spectrum of SN 1992ar is remarkably similar to a spectrum of the Type Ic SN 1983V, which as mentioned above had typical spectra. Matheson et al. (2000) interpret the one good spectrum of SN 1999cq as that of a SN Ic but with unusual (so far unique) narrow lines of He I superimposed. The spectrum of SN 1999cq certainly is peculiar.

SN 1999as probably is the brightest SN Ic known, with an absolute magnitude brighter than  $-21.4$  (Hatano et al. 2001), but since no peak apparent magnitude is available it is not included in our present sample. Its spectrum was quite unusual.

Summarizing SNe Ic: two of the three overluminous events (or three of four, counting SN 1999as) are known to have had unusual spectra. Most but not all (not SNe 1997ef and 2002ap) normal-luminosity events had typical SN Ic spectra.

## 3. Light Curves

### 3.1. Data

Light curve data in the  $V$  band were found for most of the SNe in the absolute-magnitude sample of §2. For a few events only  $R$ -band or unfiltered LC data were available. The LC data for many of the SNe were available from the same reference as the peak magnitude. In some cases we collected data from several sources in order to get as much coverage as possible. For example, most of the data for SN 1994I were taken from Richmond et al. (1996), but two late-time data points

were added from Clocchiatti et al. (1997). The SNe that have  $V$ –band LCs, with references, are listed in Table 5.

The LC data for SNe IIb/Ib and Ic are shown in Figures 3 and 4, respectively. The lines connect the symbols for each SN to help distinguish the data of one SN from another but in some cases do not depict the true shapes of the LCs.

The tails of SE SNe are powered primarily by the deposition of gamma–rays generated in the decay of  $^{56}\text{Co}$ . Because gamma–rays increasingly escape, the slopes of the LC are steeper than the  $^{56}\text{Co}$  decay slope. The only exception in the sample is SN 1984L which has a slow late–time decay slope (Figure 3).

Figures 5 and 6 are like Figures 3 and 4, respectively, except for covering a shorter time interval in order to show more detail around the time of peak brightness. The two SNe IIb LCs shown here are very similar and are less luminous than most SNe Ibc. Exceptional among the SNe Ib is the extremely luminous SN 1991D, which declined rapidly after peak. SN 1994I was very well observed and therefore often is regarded as the prototypical SN Ic, but it has the narrowest peak and the fastest overall decline among the SNe Ic of our sample.

Model fits for all of the LCs are shown in §3.2 except for SNe 1954A, 1984I, 1991N, and 2000H because the coverage in their visual LCs was too poor.

### 3.2. The Model

Numerical light–curve calculations based on hydrodynamical explosion models and various assumptions have been calculated by several groups and compared to the LCs of selected SE SNe. Here we take the approach of adopting a simple analytical model and applying it to all of the SE SNe in our sample. This results in an internally consistent set of explosion parameters (ejected mass, ejected nickel mass, and kinetic energy) for all events. The model is simple, but in view of the evidence that SE SNe tend to be aspherical, most of the numerical light–curve calculations also are oversimplified.

We use the model of Arnett (1982) for the peak of the LC, and the model of Jeffery (1999) for the tail. The Arnett model applies at early times when the diffusion approximation is valid and the Jeffery model applies at later times when the deposition of gamma–rays dominates the LC. As depicted in Figure 7 our model LC switches abruptly from the Arnett LC to the Jeffery LC when the two LCs cross. The underlying assumptions are poorest at the time of the transition. The basic assumptions are spherical symmetry; homologous expansion; that  $^{56}\text{Ni}$  is centrally concentrated rather than mixed outward in the ejecta; radiation–pressure dominance at early times; constant optical opacity at early times; and constant gamma–ray opacity at late times. The luminosity of the Arnett part is

$$L_A(t) = \epsilon_{Ni} M_{Ni} \left(10^{-\frac{\zeta}{2.5}}\right) \left(e^{-x^2}\right) \int_0^x 2ze^{(-2zy+z^2)} dz, \quad (2)$$

where  $x \equiv \frac{t}{\tau_m}$  and  $y \equiv \frac{\tau_m}{2t_{e,Ni}}$ ,

$$\tau_m = \sqrt{\frac{\kappa_{opt}}{\beta c}} \sqrt{\frac{6M_{ej}^3}{5E_k}}, \quad (3)$$

$$\epsilon_{Ni} = \frac{Q_{ph+PE}^{Ni}}{m_{Ni} t_{e,Ni}} \quad (4)$$

The luminosity of the Jeffery part is:

$$L_J(t) = \epsilon_{Ni} M_{Ni} \left\{ e^{-\frac{t}{t_{e,Ni}}} + G \left( e^{-\frac{t}{t_{e,Co}}} - e^{-\frac{t}{t_{e,Ni}}} \right) \left[ f_{PE}^{Co} + f_{ph}^{Co} \left( 1 - e^{-\left(\frac{t_0}{t}\right)^2} \right) \right] \right\}, \quad (5)$$

where

$$t_0 = \sqrt{\frac{M_{ej}\kappa_\gamma}{4\pi v_a v_b}}, \quad (6)$$

$$v_i = v_i^{93J} \sqrt{\frac{\left(\frac{E_k}{M_{ej}}\right)}{\left(\frac{E_k}{M_{ej}}\right)_{93J}}}, \quad i = a, b, \quad (7)$$

$$G = \left( \frac{Q_{ph+PE}^{Co}}{Q_{ph+PE}^{Ni}} \right) \left( \frac{m_{Ni}}{m_{Co}} \right) \left( \frac{t_{e,Ni}}{t_{e,Co} - t_{e,Ni}} \right) = 0.184641. \quad (8)$$

The e-folding times for  $^{56}\text{Co}$  and  $^{56}\text{Ni}$  decay,  $t_{e,Co}$  and  $t_{e,Ni}$ , are 111 and 8.77 days, respectively. The energy per decay, including energy from photons and electron–positron pairs but not from neutrinos (which escape), are  $Q_{ph+PE}^{Co} = 3.74$  MeV and  $Q_{ph+PE}^{Ni} = 1.73$  MeV. For  $^{56}\text{Co}$  decay the fractions of energy in photons  $f_{ph}$  and in kinetic energy of positron  $f_{PE}$  are 0.968 and 0.032, respectively. The above quantities are from Table 1 of Jeffery (1999). The optical and gamma-ray opacities are taken to be  $\kappa_{opt} = 0.4 \text{ cm}^2 \text{ g}^{-1}$  and  $\kappa_\gamma = 0.04 \text{ cm}^2 \text{ g}^{-1}$ . Arnett (1982) defined  $\beta$  as  $4\pi(\alpha I_M/3)$ , where  $\alpha I_M = 3.29$  for uniform density (Arnett 1980).

The model LC is bolometric.  $V$ –band LCs are generally regarded as having similar shape, but in order to adjust the brightness of the model to better match a  $V$ –band LC a correction  $\zeta$  was used for the Arnett part of the LC. The value of  $\zeta$  was determined by calibrating the peak of the LC to that of a typical SN Ia. This was done by fixing  $E_k$  to 1 foe ( $10^{51}$  erg),  $M_{ej}$  to  $1.4 M_\odot$ , and  $M_{Ni}$  to  $0.6 M_\odot$ , then choosing  $\zeta = -1.48$  so that the peak absolute magnitude became  $-19.5$ .

The velocities  $v_a$  and  $v_b$  are the inner and outer velocities within which the mass density can be regarded as roughly constant. Jeffery (1999) used velocities thought to be appropriate for SN 1987A. A better approximation for SE SNe is to use velocities thought to be appropriate for SN 1993J (the most thoroughly observed and modeled SE SN) and to rescale these velocities with respect to  $E_k/M_{ej}$  for each SN (equation 7). For SN 1993J we use  $v_a = 1000 \text{ km s}^{-1}$ ,  $v_b = 10,000 \text{ km s}^{-1}$ , and  $(E_k/M_{ej})_{93J} = 0.51 \text{ foe}/M_\odot$ , from Blinnikov et al. (1998).

We began our study with four adjustable model parameters:  $E_k$ ,  $M_{ej}$ ,  $M_{Ni}$ , and  $t_{shift}$ , where  $t_{shift}$  shifts the LC on the time axis. The best  $\chi^2$  fit often was formally very good but the model parameters were physically unreasonable. To remedy this problem we developed the following procedure for constraining the  $E_k/M_{ej}$  ratio using spectroscopic information. We used the parameterized supernova synthetic-spectrum code **Synow** (Branch et al. 2002) to construct a relation between the wavelength of the peak of an Fe II blend near 5000 Å and the **Synow** input parameter  $v_{phot}$ , the velocity at the photosphere (Figure 8). We measured the wavelength of the peak in spectra of each event and obtained a value of  $v_{phot}$  from Figure 8. We defined  $a(t) = (E_k/M_{ej})/v_{phot}^2(t)$  and used values of  $E_k/M_{ej}$  obtained by others from numerical LC calculations for seven events of our sample (references are in Table 6) to construct Figures 9 and 10, for normal-luminosity SE SNe and hypernovae, respectively. In these figures the dashed line is the adopted relation and the difference between the dashed line and the solid lines is taken as the uncertainty. For the remaining events of the sample (those not having  $E_k/M_{ej}$  values from numerical LC calculations), we used Figures 9 and 10 with our estimates of  $v_{phot}(t)$  to obtain estimates of  $E_k/M_{ej}$ .

With  $E_k/M_{ej}$  thus estimated spectroscopically, and three rather than four adjustable model parameters we obtained relatively good fits with reasonable parameter values (in most cases).

### 3.3. Results

The parameter values determined from the best model fits are listed in Table 6. Because uncertainties are not available for each data point in all LCs, we quote the uncertainty at peak,  $\delta M_V$ , as the characteristic uncertainty. The uncertainties in  $M_V$  given in Table 6 differ from those listed in Tables 1 – 3 because here each one has the uncertainty in  $E_k/M_{ej}$  added in quadrature.

About half of the SNe modeled here have been modeled in similar studies; most by more sophisticated numerical models. Since our model is an analytic model, it has the advantage of being fast and therefore, we can use it on a larger sample. Table 7 gives a comparison of our results to the results of the other studies. The values of  $M_{ej}$  from these other models tend to be larger than ours by a factor of approximately two.

Since at least some, if not all, hypernovae are associated with GRBs there is likely some interaction between the GRB jet and the expanding SN shell. A first order approximation is to say that the SN occurs independent of the GRB. For our simple model this is a reasonable approximation.

### 3.3.1. Type IIb

SN 1993J is the only SE SN that has been observed early enough to see the break-out shock in the  $V$ –band LC. Because the break-out shock has not been incorporated into the model we are using, that part of the LC has been omitted from our analysis. The model fit for SN 1993J (Figure 11a), with  $E_k = 0.66$  foe and  $M_{ej} = 1.3 M_\odot$ , looks satisfactory although  $\chi^2 = 2.14$  is somewhat large and probably due to the small adopted value of  $\delta M_V$ . Numerical LC calculations were carried out by Young, Baron, & Branch (1995) and Blinnikov et al. (1998): the former imposed  $E_k = 1$  foe and favored a model having  $M_{ej} = 2.6 M_\odot$ ; the latter adopted a model having  $E_k = 1.2$  foe and obtained a fit with  $M_{ej} = 2.45 M_\odot$ . If we impose  $E_k = 1$  foe and let  $M_{ej}$  vary, we get  $M_{ej} = 1.6 M_\odot$  (Table 7).

The model fit for SN 1996cb (Figure 11b), with  $E_k = 0.22$  foe and  $M_{ej} = 0.9 M_\odot$ , is slightly too dim at the peak but overall it is satisfactory.

### 3.3.2. Type Ib

Of the seven SNe Ib LCs plotted in Figure 3, five are worth fitting. The model fit to the fragmentary LC of SN 1983N (Figure 12a), with  $E_k = 0.30$  foe and  $M_{ej} = 0.8 M_\odot$ , is good. We were not able to obtain an acceptable fit to the entire LC of SN 1984L (see figure 13b) because of the exceptionally slow decline in the tail (Figure 3). However, when the data obtained later than 200 days after explosion were omitted, we did obtain a satisfactory fit (Figure 12c), with  $E_k = 0.97$  foe and  $M_{ej} = 1.8 M_\odot$  (this result is denoted “pk” in Table 6). Baron, Young, & Branch (1993) also had trouble fitting all of the data with detailed LC calculations, and were forced to what they regarded as an improbable model having a very small optical opacity and  $E_k \simeq 20$  foe,  $M_{ej} \simeq 50 M_\odot$ .

The LC of SN 1990I (Figure 12d) drops rapidly after 250 days and our best fitting model, which has  $E_k = 0.67$  foe and  $M_{ej} = 1.2 M_\odot$ , cannot account for this. The problem with the fit near peak brightness is due to the compromise between trying to fit the tail and the peak. If the data later than 250 days are ignored, we get a better fit with only slight changes in the model parameters.

SN 1991D, the brightest SN in the sample, has an exceptional LC that declines rapidly from the peak, yet from its spectra we obtain  $E_k/M_{ej} = 0.13$  foe/ $M_\odot$ , the smallest value in the sample. The model cannot reconcile these contradictory aspects (Figure 12e). It is possible to get a good fit if we drop the constraint on the  $E_k/M_{ej}$  ratio, but then we obtain  $E_k/M_{ej} = 8$  foe/ $M_\odot$  which is inconsistent with the spectra. Benetti et al. (2002) used a semi-analytical model to fit the LC of SN 1991D. They suggested this peculiar event may have been a SN Ia exploding inside the extended helium-rich envelope of a companion star. If this is correct then although SN 1991D must be regarded as Type Ib according to SN spectral classification, physically it may have more

in common with SNe Ia.

SN 1999ex has very good coverage around the peak but there are no data for the tail. The model fit, with  $E_k = 0.30$  foe and  $M_{ej} = 0.9 M_\odot$ , is satisfactory.

Other studies have looked at the LCs of SN 1983N (Shigeyama et al. 1990) and SN 1990I (Elmhamdi et al. 2004) assuming  $E_k = 1$  foe. Their results are listed in Table 7 along with our results for comparison; as well as what we found when we imposed  $E_k = 1$  foe. In both cases our value for  $M_{ej}$  was somewhat smaller and is increased when imposing  $E_k = 1$  foe.

### 3.3.3. Type Ic

Model fits were carried out for all of the SN Ic LCs plotted in Figure 4 except for SN 1991N. The fit for the limited LC of SN 1962L, with  $E_k = 0.11$  foe and  $M_{ej} = 0.6 M_\odot$ , is satisfactory (Figure 13a).  $M_{Ni} = 0.37$  is more than half as high as  $M_{ej}$ . The very low  $\chi^2$  is due to the large uncertainty of  $\delta M_V = 0.85$ .

For SN 1983I (Figure 13b) there are no pre-peak data. Our fit, with  $E_k = 0.33$  foe and  $M_{ej} = 0.7 M_\odot$ , is satisfactory. Our fit to the fragmentary LC of SN 1983V (Figure 13c) is satisfactory, with  $E_k = 0.99$  foe and  $M_{ej} = 1.3 M_\odot$ . Our fit to the fragmentary LC of SN 1987M also is satisfactory (Figure 13d), with  $E_k = 0.19$  foe and  $M_{ej} = 0.4 M_\odot$ .

The fit for SN 1990B (Figure 13e), with  $E_k = 0.55$  foe and  $M_{ej} = 0.9 M_\odot$  fits the date well except for the last data point. According to Clocchiatti et al. (2001) that point is especially uncertain because of the difficulty of subtracting the host galaxy light. SN 1992ar is the brightest SN Ic in the sample. The model fit (Figure 13f), with  $E_k = 1.1$  foe,  $M_{ej} = 1.5 M_\odot$ , and a high value of  $M_{Ni} = 0.84 M_\odot$ , is acceptable.

SN 1994I has a very narrow LC peak and the best model fit (Figure 14a), with  $E_k = 0.55$  foe and  $M_{ej} = 0.5 M_\odot$ , is too broad at peak. Thus the value of  $t_{rise}$  given in Table 6, which already is the smallest value in the sample, is too large.

The last three LCs are those of three hypernovae. As mentioned above, these are SE SNe that have very broad, blueshifted absorption features at early times. The LC of SN 1997ef, which has a very broad peak and appears to have a very late transition point (Figure 14b), is not well fit by our model, which gives  $E_k = 3.3$  foe and  $M_{ej} = 3.1 M_\odot$ . The model fit for SN 1998bw (Figure 14c), with  $E_k = 31$  foe and  $M_{ej} = 6.2 M_\odot$ , is good except near the transition point. This is by far the highest value of  $E_k$  for the events of the sample. Figure 14d shows the fit for SN 2002ap, with  $E_k = 2.7$  foe and  $M_{ej} = 1.7 M_\odot$ . Overall it is not bad, although the model peak is a bit dim and the model transition point is somewhat early. The model has trouble finding a tail that fits both the transition point and the two late time data points.

Other studies have looked at the LCs of SN 1983I (Shigeyama et al. 1990) and SN 1987M

(Nomoto, Filippenko, & Shigeyama 1990) assuming  $E_k = 1$  foe. Their results are listed in Table 7 along with our results for comparison; as well as what we found when we imposed  $E_k = 1$  foe. In both cases our value for  $M_{ej}$  was somewhat smaller, but increased when imposing  $E_k = 1$  foe.

We compare our results for the three hypernovae with the results of other studies in Table 7. The value of  $E_k$  given in Table 6 for the brightest of the three (SN 1998bw) is comparable to the values found by Nakamura et al. (2001) ( $E_k = 50$  foe) and Woosley, Eastman, & Schmidt (1999) ( $E_k = 22$  foe). The dimmest of the three hypernovae (SN 1997ef) is compared to a study by Iwamoto et al. (2000) where they obtained  $E_k = 8$  foe and  $M_{ej} = 7.6M_\odot$ .

#### 4. Summary

We have used the available data to characterize the absolute-magnitude distributions of the SE SNe in the current observational sample. Most SE SNe have a “normal” luminosity, which at  $M_V = -17.77 \pm 0.06$  is about a magnitude and a half dimmer than SNe Ia. One sixth of the current sample of SE SNe are overluminous, i.e., more luminous than SNe Ia, but these are strongly favored by observational selection so the true fraction of SE SNe that are overluminous is much lower than one sixth. The small size of the sample and the considerable absolute magnitude uncertainties, especially those due to host galaxy extinction, still prevent an absolute magnitude difference between SNe Ib and Ic from being firmly established. Three of the four (or four of the five, counting SN 1999as) overluminous SE SNe are known to have had unusual spectra; a few of the normal-luminosity SE SNe also had unusual spectra. Much more data on SE SNe are needed in order to better determine the absolute-magnitude distributions, and to correlate absolute magnitudes with spectroscopic characteristics.

Absolute light curves in the  $V$  band (some fragmentary) are available for two SNe IIb, seven SNe Ib, and 12 SNe Ic including three hypernovae. Two of the SNe Ib, SNe 1984L and 1991D, have LCs that are quite different from those of the others. The light curves of the SNe Ic are rather diverse. The light curve of SN 1994I, often considered to be a typical SN Ic, actually is the most rapidly declining light curve in the SN Ic sample.

The simple analytical light-curve model was applied to two SNe IIb, five SNe Ib and 10 SNe Ic. Instead of assuming a kinetic energy, such as the canonical one foe, an  $E_k/M_{ej}$  ratio was estimated on the basis of spectroscopy, and the model fits then produced internally consistent values of  $E_k$ ,  $M_{ej}$ , and  $M_{Ni}$ .

Reasonably good fits were obtained for the two SNe IIb and three of the five SNe Ib. The slowly decaying tail of the SN 1984L LC and the rapid decline from the peak of the SN 1991D LC cannot be fit by the model. With the exception of the hypernova SN 1997ef, reasonable fits were obtained for the SNe Ic, with a considerable range in the parameter values. As expected, the hypernovae have high  $E_k$  and somewhat high  $M_{ej}$ , but only one of the three has high  $M_{Ni}$ .

Our values of  $M_{ej}$  (and  $E_k$ ) tend to be lower than those obtained by others by means of numerical LC calculations, while our values for  $M_{Ni}$  are a little higher. Some of the other numerical calculations are based on an assumed canonical value of  $E_k = 1$  foe. Because our spectroscopic constraint on  $E_k/M_{ej}$  together with our LC model leads to lower  $E_k$ , and lower  $E_k$  makes the LC peak dimmer, we need slightly higher  $M_{Ni}$  values to make the LC peaks as bright as observed.

The diversity among SN Ic LCs is of special interest in connection with the ongoing search for SN signals in GRB afterglows. In a forthcoming paper we will apply the same modeling technique used in this paper to the putative SN bumps in GRB afterglow light curves. This will enable us to infer internally consistent SN parameter values for comparison with the results of this paper, and to investigate the issue of whether the GRBs and the associated SNe are coincident in time or whether, as in the supranova model, the SN precedes the gamma-ray burst.

We would like to thank Rollin C. Thomas for helpful comments and suggestions. Support for this work was provided by NASA through grants GO-09074 and GO-09405 from the Space Telescope Science Institute, which is operated by the Association of Universities for Research in Astronomy, Inc., under NASA contract NAS 5-25255. Additional support was provided by National Science Foundation grants AST-9986965 and AST-0204771.

## REFERENCES

- Arnett, D. 1980, *ApJ*, 237, 541
- Arnett, D. 1982, *ApJ*, 253, 785
- Ayani, K., R. Furusho, R., Kawakita, H., Fujii, M., & Yamaoka, H. 1999, IAUC7244
- Barbon, R., Benetti, S., Cappellaro, E., Pata, F., Turatto, M., & Iijima, T. 1995, *A&AS*, 110, 513
- Barbon, R., Buondi, V., Cappellaro, E., & Turatto, M. 1999, *A&AS*, 139, 531
- Baron, E., Young, T., & Branch, D. 1993, *ApJ*, 409, 417
- Barth, A. J., van Dyk, S., Filippenko, A., Leibundgut, B., & Richmond, M. 1996, *AJ*, 111, 2047
- Benetti, S., Cappellaro, E., Turatto, M., & Pastorello, A. 2000, IAUC7375
- Benetti, S., Branch, D., Turatto, M., Cappellaro, E., Baron, E., Zampieri, L., Della Valle, M., & Pastorello, A., 2002, *MNRAS*, 336, 91
- Bertola, F. 1964, *Ann. Astrophys.*, 27, 319
- Blinnikov, S., Eastman, R., Bartunov, O., Popolitov, V., & Woosley, S. 1998, *ApJ*, 496, 454
- Branch, D., et al. 2002, *ApJ*, 566, 1005
- Branch, D. 2003, *A Massive Star Odyssey, from Main Sequence to Supernova*, Proc. IAU Symposium NO 212, eds. K. A. van der Hucht, A. Herrero, & C. Estaban (San Francisco: Astronomical Society of the Pacific), p. 346
- Clocchiatti, A., Wheeler, J. C., Benetti, S., & Frueh, M. 1996, *ApJ*, 459, 547
- Clocchiatti, A., et al. 1997, *ApJ*, 483, 675
- Clocchiatti, A., et al. 2000, *ApJ*, 529, 661
- Clocchiatti et al. 2001, *ApJ*, 553, 886
- Drozdovsky, I., Schulte-Ladbeck, R., Hopp, U., Greggio, L., & Crone, M. 2002, *AJ*, 124, 811
- Elmhamdi, A., Danziger, I. J., Cappellaro, E., Della Valle, M., Gouffes, C., Phillips, M. M., & Turatto, M. 2004, *A&A*, 426, 963
- Feldmeier, J., Ciardullo, R., & Jacoby, G. 1997, *ApJ*, 479, 231
- Filippenko, A. 1987, IAUC4428
- Filippenko, A. 1988, *AJ*, 96, 1941

- Filippenko, A., Porter, A., & Sargent, W. 1990, AJ, 100, 1575
- Foley, R., et al. 2003, PASP, 115, 1220
- Freedman, W., et al. 2001, ApJ, 553, 47
- Galama, T., et al. 1998, Nature, 395, 670
- Galama, T., et al. 1999, A&AS, 138, 465
- Gal-Yam, A., Ofek, E., & Shemmer, O. 2002 MNRAS, 332L, 73
- Garnavich, P., Matheson, T., Olszewski, E. W., Harding, P., & Stanek, K. Z. 2003, IAUC8114
- Grothues, H. G., & Schmidt-Kaler, T. 1991, A&A, 242, 357
- Harkness, R., et al. 1987, ApJ, 317, 355
- Hamuy, M., et al. 2002, AJ, 124, 417
- Hatano, K., Branch, D., Nomoto, K., Deng, J. S., Maeda, K., Nugent, P., & Aldering, G. 2001, BAAS, 198, 3902
- Homeier, N. L. 2005, ApJ, 620, 12
- Iwamoto, K., et al. 2000, ApJ, 534, 660
- Jeffery, D. 1999, preprint (astro-ph/9907015)
- Jha, S., Garnavich, P., Challis, P., & Kirshner, R. 1998, IAUC7011
- Kantowski, R., Kao, J., & Thomas, R. C. 2000, ApJ, 545, 549
- Kinugasa, K., et al. 2002, ApJ, 577L, 97
- Klose, S., Guenther, E., & Woitas, J. 2002, GCN, 1248, 1
- Korth, S. 1991a, IAUC5234
- Korth, S. 1991b, IAUC5251
- Krisciunas, K., & Rest, A. 2000, IAUC7382
- Kulkarni, S., Bloom, J., Frail, D., Ekers, R., Wieringa, M., Wark, R., & Higdon, J. 1998, IAUC6903
- Leibundgut, B., Phillips, M. M., & Graham, J. A. 1990, PASP, 102, 898
- Leibundgut, B., Tammann, G. A., Cadonau, R., & Cerrito, D. 1991, A&AS, 89, 537
- Lewis, J., et al. 1994, MNRAS, 266, L27

- Matheson, T., Filippenko, A., Chornock, R., Leonard, D., & Li, W. 2000, AJ, 119, 2303
- Matheson, T., Filippenko, A., Li, W., Leonard, D., & Shields, J. 2001, AJ, 121, 1648
- Maza, J., & Ruiz, M.T. 1989, ApJS, 69, 353
- Mazzali, P., Iwamoto, K., & Nomoto, K. 2000 ApJ, 545, 407
- Mazzali, P., et al. 2002, ApJ, 572, L61
- McKenzie, E., & Schaefer, B. 1999, PASP, 111, 964
- Nakamura, T., Mazzali, P., Nomoto, K., & Iwamoto, K. 2001, ApJ, 550, 991
- Nomoto, K., Filippenko, A., & Shigeyama, T. 1990, A&A, 240, L1
- Pandey, F., Anupama, G., Sagar, R., Bhattacharya, D., Sahu, D., & Pandey, J. 2003, MNRAS, 340, 375
- Patat, F., et al. 2001, ApJ, 555, 900
- Phillips, M. M., & Graham, J. A. 1984, IAUC3946
- Phillips, M., & Hamuy, M. 1992, IAUC5574
- Porter, A., & Filippenko, A. 1987, AJ, 93, 1372
- Qiu, Y., Li, W., Qiao, Q., & Hu, J. 1999, AJ, 117, 736
- Richardson, D., Branch, D., Casebeer, D., Millard, J., Thomas, R. C., & Baron, E. 2002, AJ, 123, 745 (R02)
- Richmond, M., Treffers, R., Filippenko, A., Paik, Y., Leibundgut, B., Schulman, E., & Cox, C. 1994, AJ, 107, 1022
- Richmond, M., et al., 1996, AJ, 111, 327
- Saha, A., Sandage, A., Tamman, G. A., Dolphin, A. E., Christensen, J., Panagia, N., & Macchetto, F. D. 2001, ApJ, 562, 314
- Schaefer, B. 1995, ApJ, 450, L5
- Schaefer, B. 1996, ApJ, 464, 404
- Schlegel, D., & Kirshner, R. 1989, AJ, 98, 577
- Schlegel, D., Finkbeiner, D., & Davis, M. 1998, ApJ, 500, 525
- Shigeyama, T., Nomoto, K., Tsujimoto, T., & Hashimoto, M. 1990, ApJ, 361, L23

- Sollerman, J., Kozma, C., Fransson, C., Leibundgut, B., Lundqvist, P., Ryde, F., & Woudt, P. 2000, *ApJ*, 537, L127
- Stritzinger, M., et al. 2002, *AJ*, 124, 2100
- Thim, F., Tammann, G. A., Saha, A., Dolphin, A., Sandage, A., Tolstoy, E., & Labhardt, L. 2003, *ApJ*, 590, 256
- Tsvetkov, D. 1985, *Astron. Ah.*, 62, 365
- Tsvetkov, D. 1994, *Astronomy Reports*, 38, 74
- Tully, R. B. 1988, *Nearby Galaxies Catalog* (Cambridge: Cambridge University Press)
- Turatto, M., Benetti, S., & Cappellaro, E. 2003, *From Twilight to Highlight – The Physics of Supernovae*, ESO/MPA/MPE Workshop Garching, ed. W. Hillebrandt & B. Leibundgut (Berlin: Springer), p. 200 (astro-ph/0211219)
- van Driel, W., et al. 1993, *PASJ*, 45, L59
- Wellmann, P., & Beyer, M. 1955, *Z. Astrophysics*, 35, 205
- Wheeler, J. C., & Levreault, R. 1985, *ApJ*, 294, L17
- Woosley, S., Eastman, R., & Schmidt, B. 1999, *ApJ*, 516, 788
- Yoshii, Y., et al. 2003, *ApJ*, 592, 467
- Young, T., Baron, E., & Branch, D. 1995, *ApJ*, 449, L51

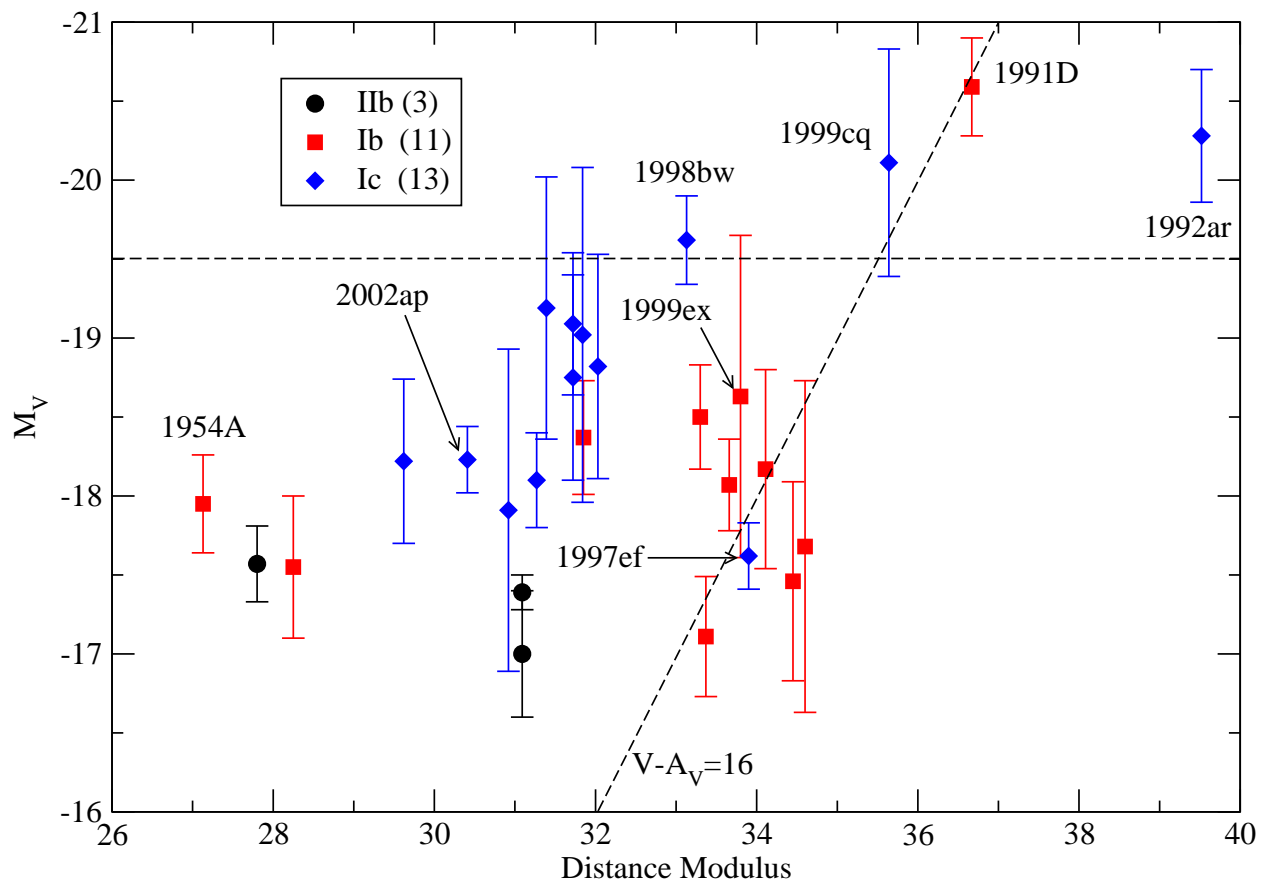


Fig. 1.— Absolute visual magnitude versus distance modulus with the vertical error bars shown. Some key SNe are labeled.

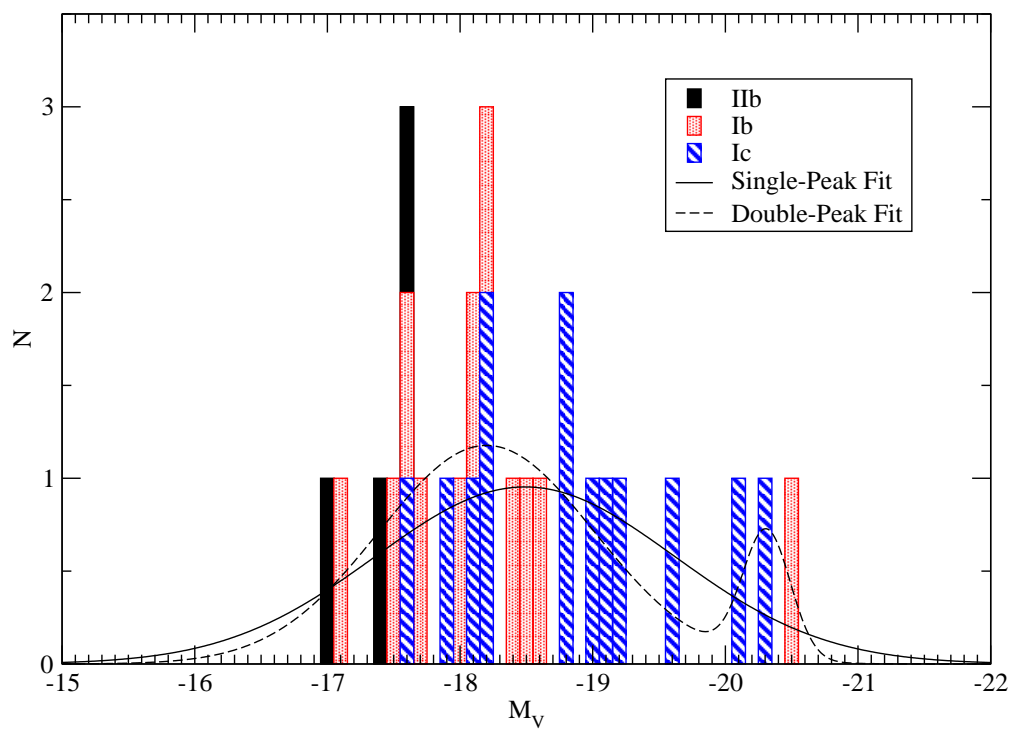


Fig. 2.— A histogram of SE SN absolute magnitudes, with 0.1 magnitude bin width. The best single-Gaussian and double-Gaussian fits (see text) are also shown.

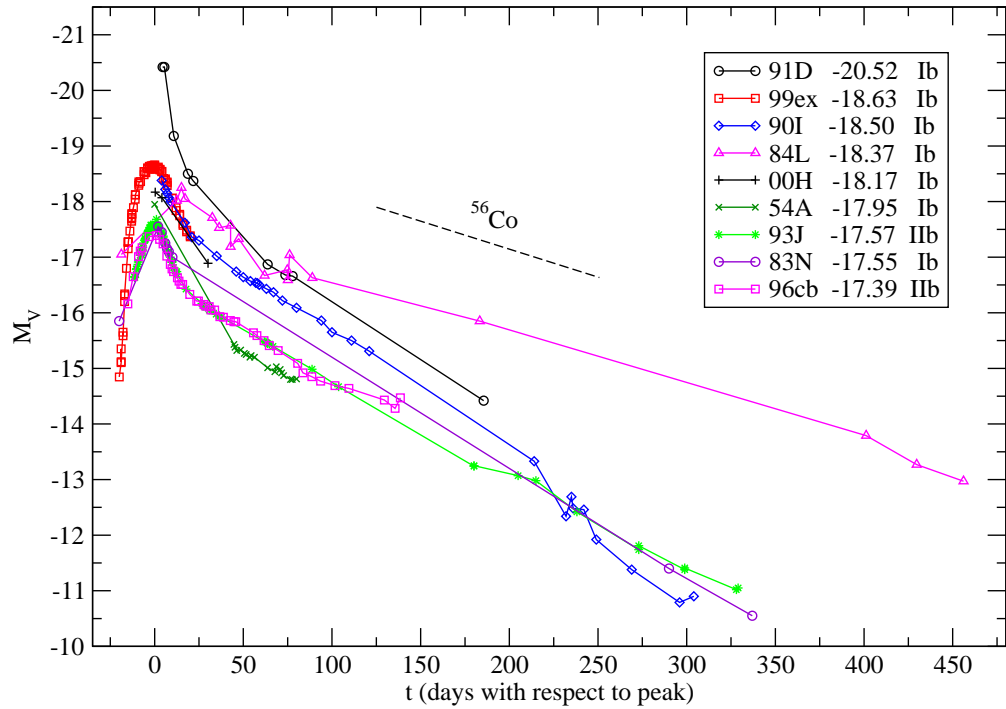


Fig. 3.— The absolute light curves are plotted for SNe IIb and Ib. The peak absolute magnitudes are given in the legend. The  $^{56}\text{Co}$  decay slope is shown for reference. Solid lines are only to guide the eye.

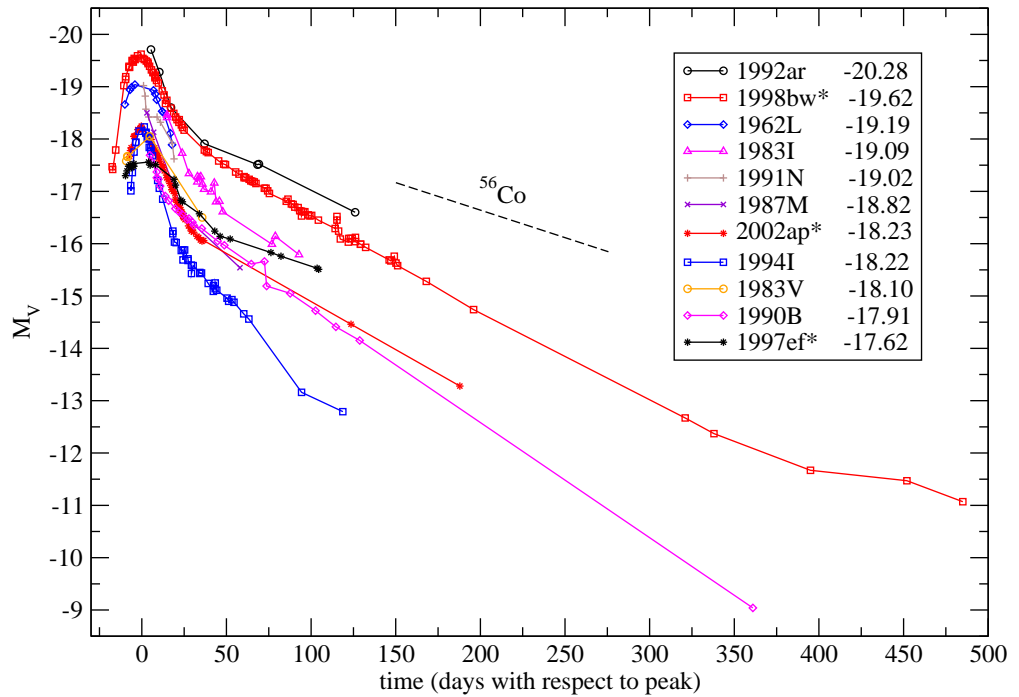


Fig. 4.— The absolute light curves are plotted for SNe Ic. The peak absolute magnitudes are given in the legend. The  $^{56}\text{Co}$  decay slope is shown for reference. Solid lines are only to guide the eye. (\*=hypernovae)

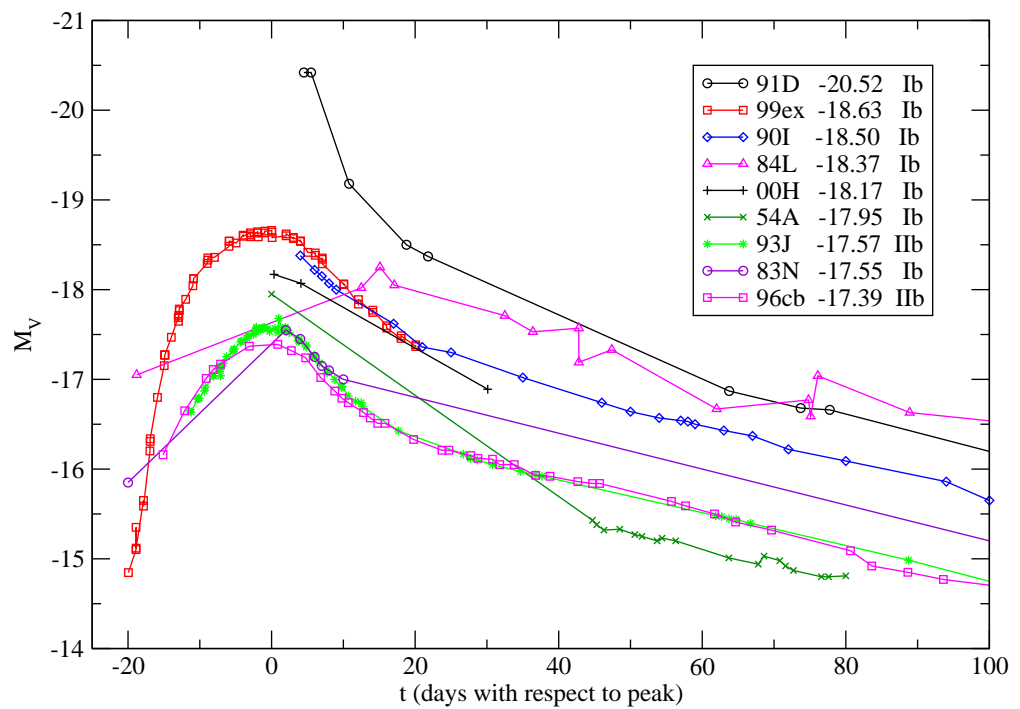


Fig. 5.— Same as Figure 3, except shown on a smaller time scale around peak brightness.

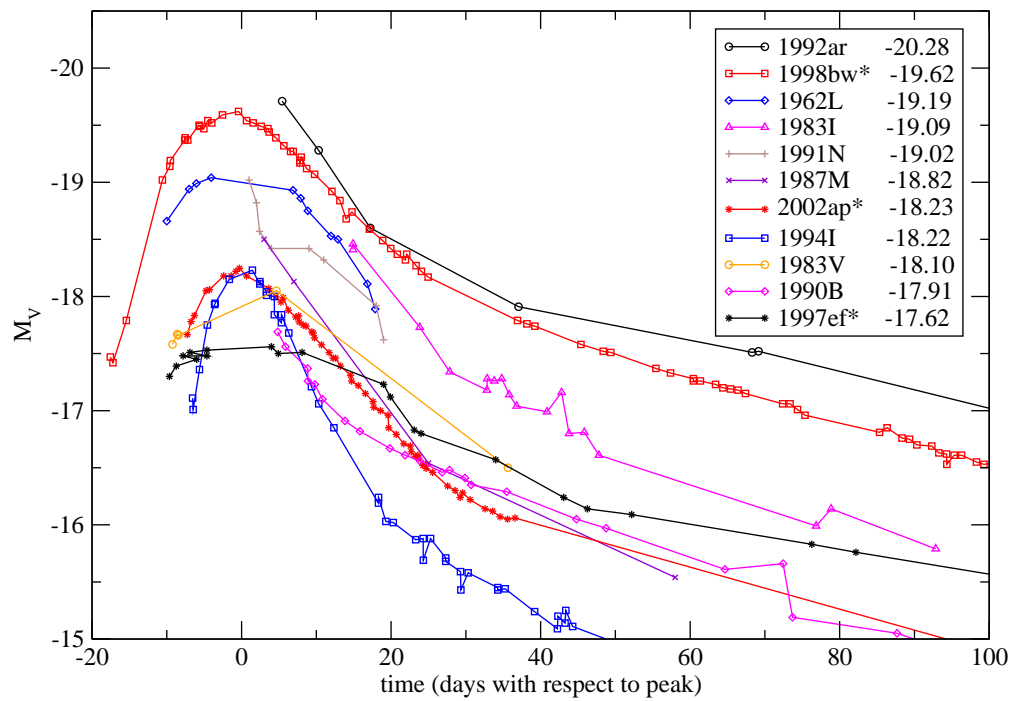


Fig. 6.— Same as Figure 4, except shown on a smaller time scale around peak brightness. (\*=hypernovae)

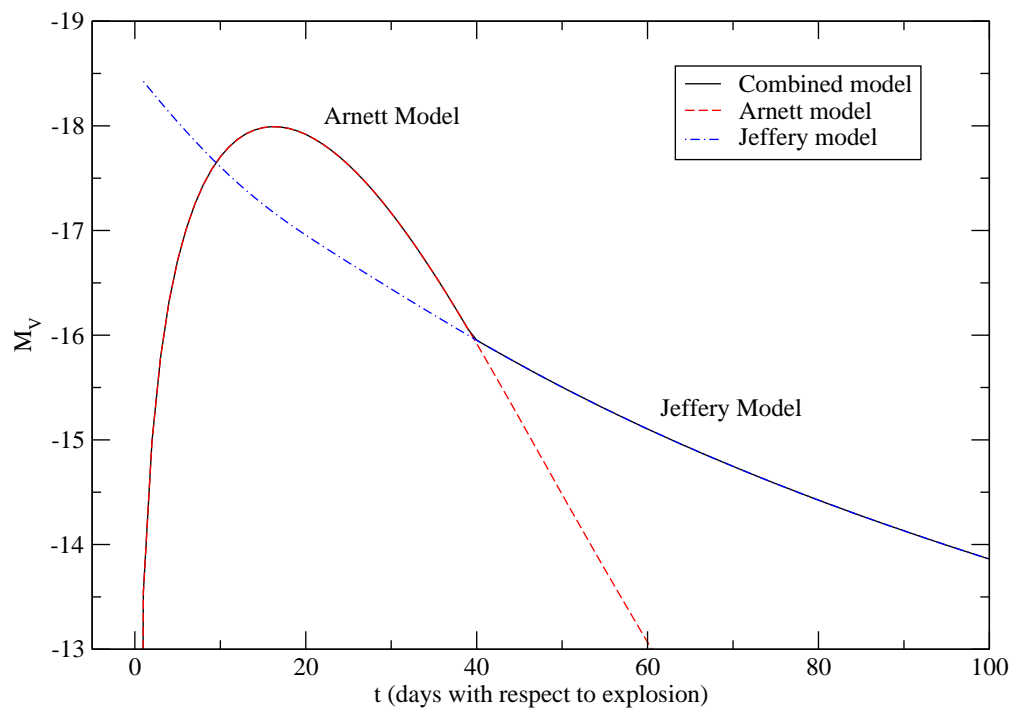


Fig. 7.— Here the combined model is shown by the solid line and the Arnett and Jeffery models are shown as dashed lines.

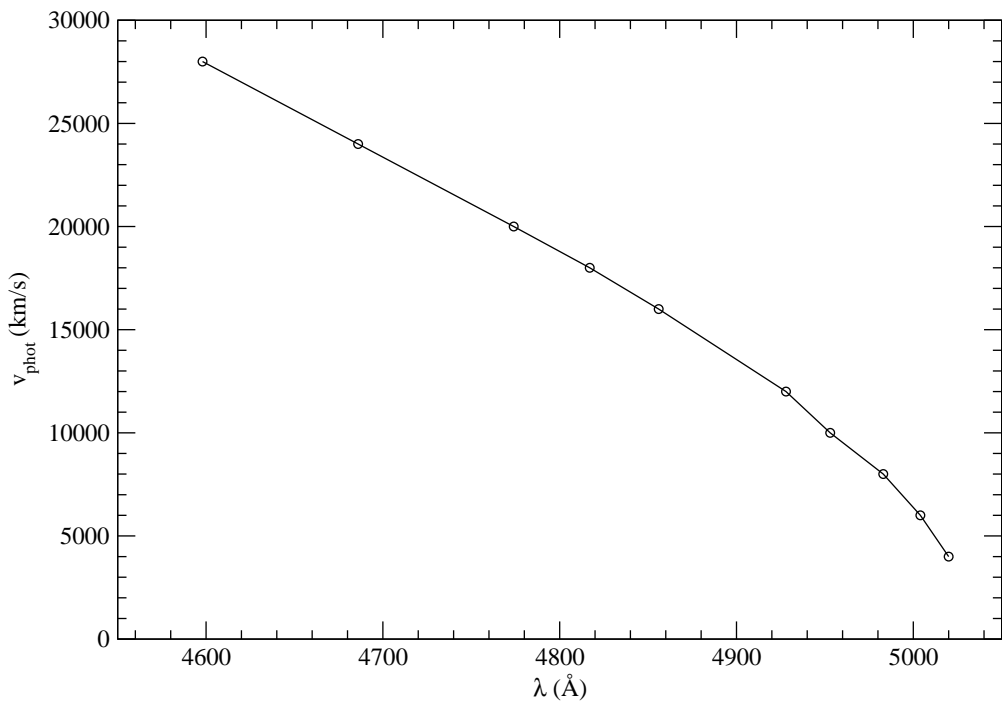


Fig. 8.— The relation between  $v_{\text{phot}}$  and the peak of the FeII blend near 5000Å are shown as determined by **Synow**.

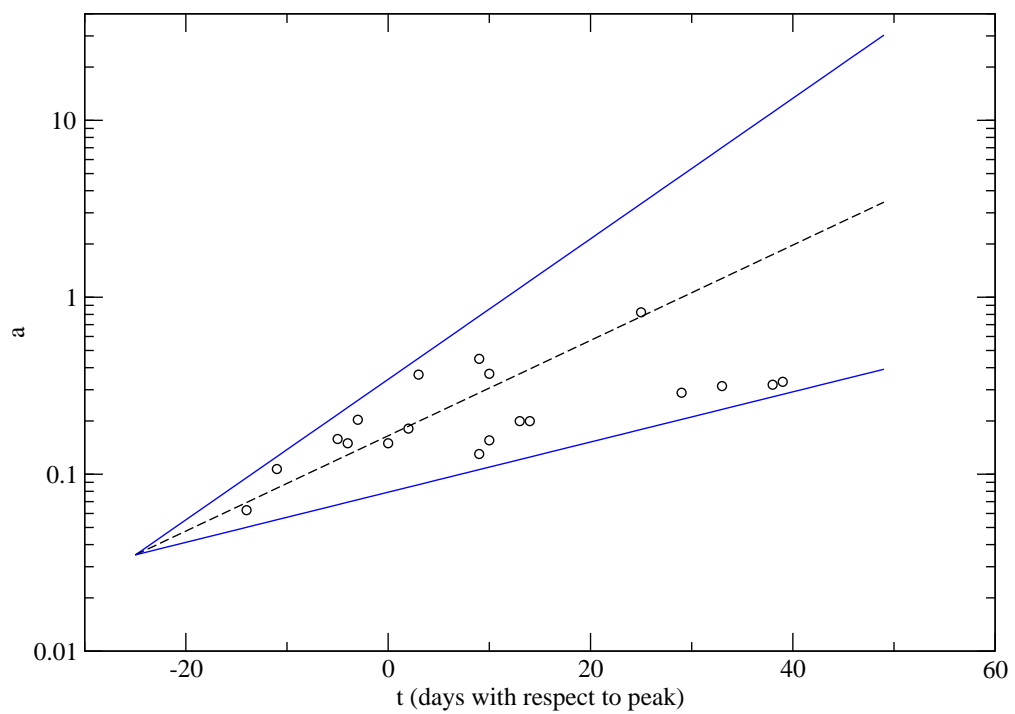


Fig. 9.— For normal SE SNe,  $a(t)$  is shown on a log scale with solid lines showing the upper and lower limits and the dashed line showing the mean.

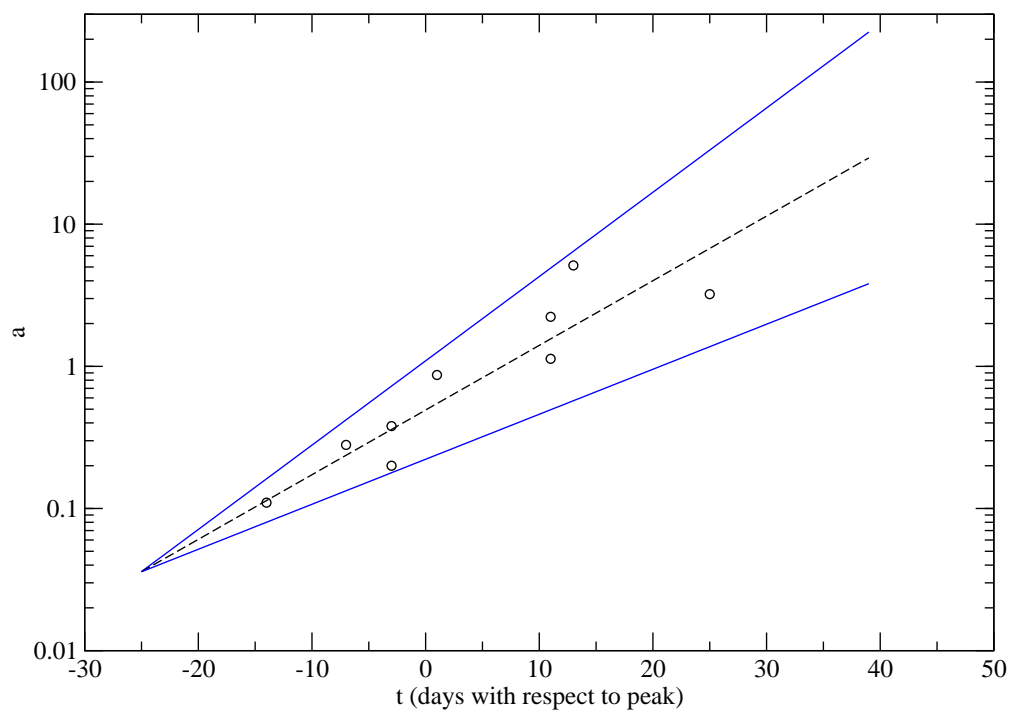


Fig. 10.— For hypernovae,  $a(t)$  is shown on a log scale with solid lines showing the upper and lower limits and the dashed line showing the mean.

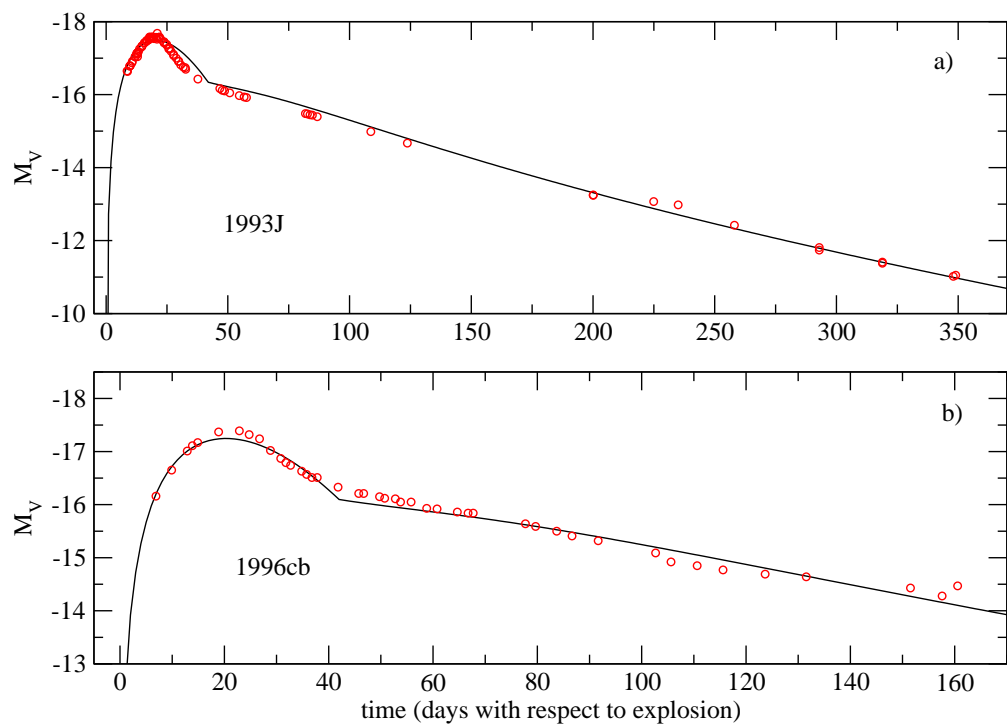


Fig. 11.— The best fit for the SNe IIb (graphs are scaled independently).

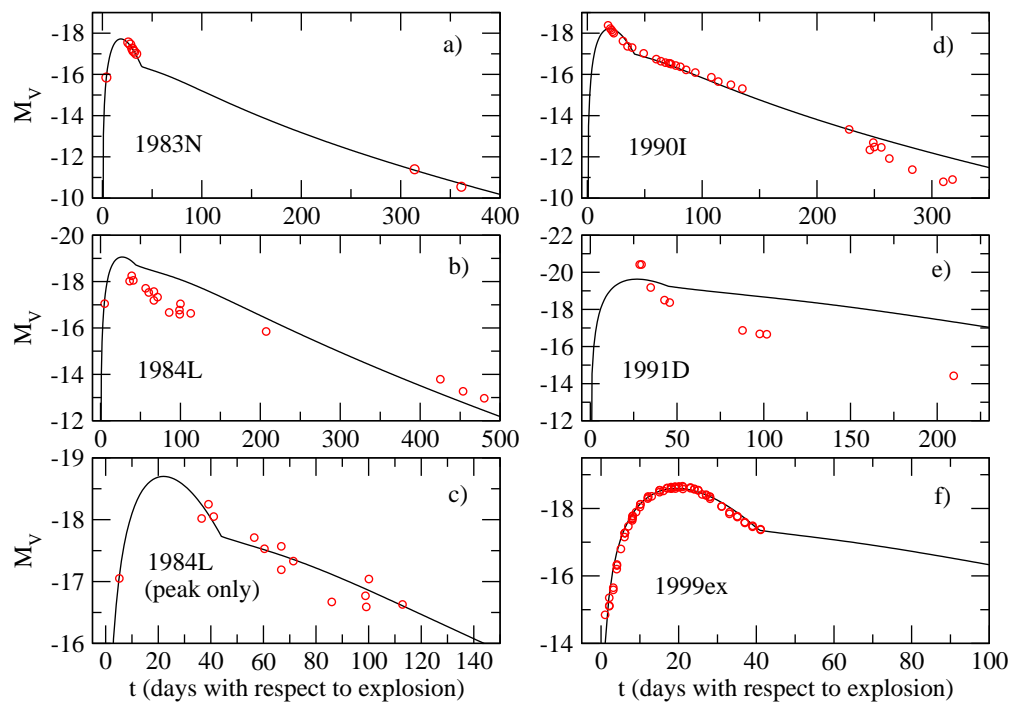


Fig. 12.— The best fit for the SNe Ib (graphs are scaled independently).

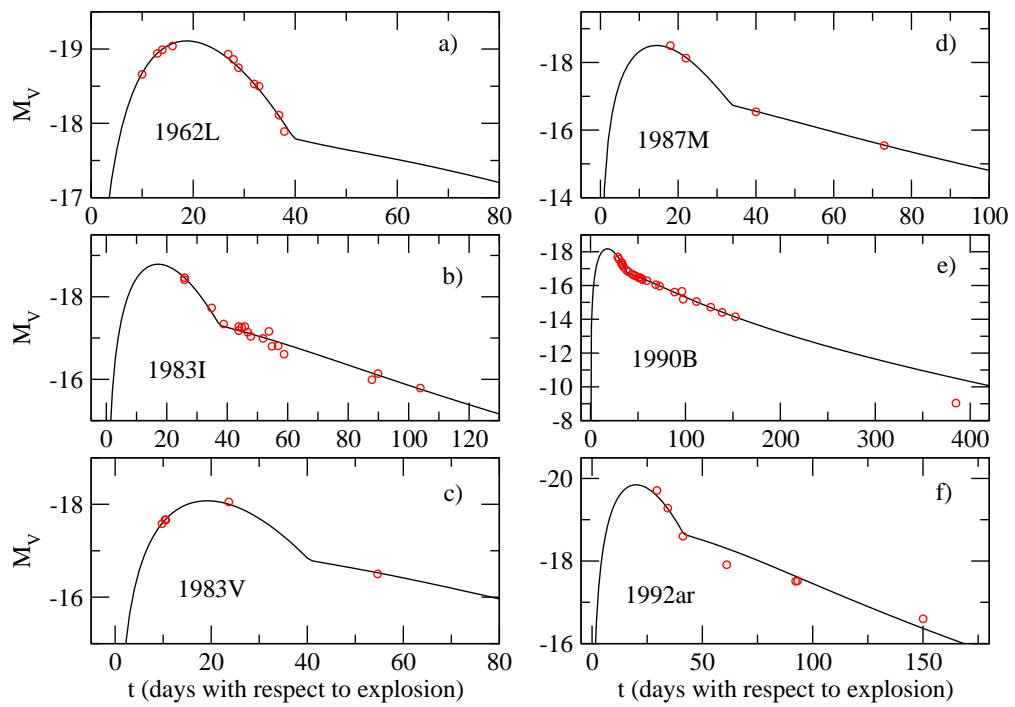


Fig. 13.— The best fit for SNe Ic (graphs are scaled independently).

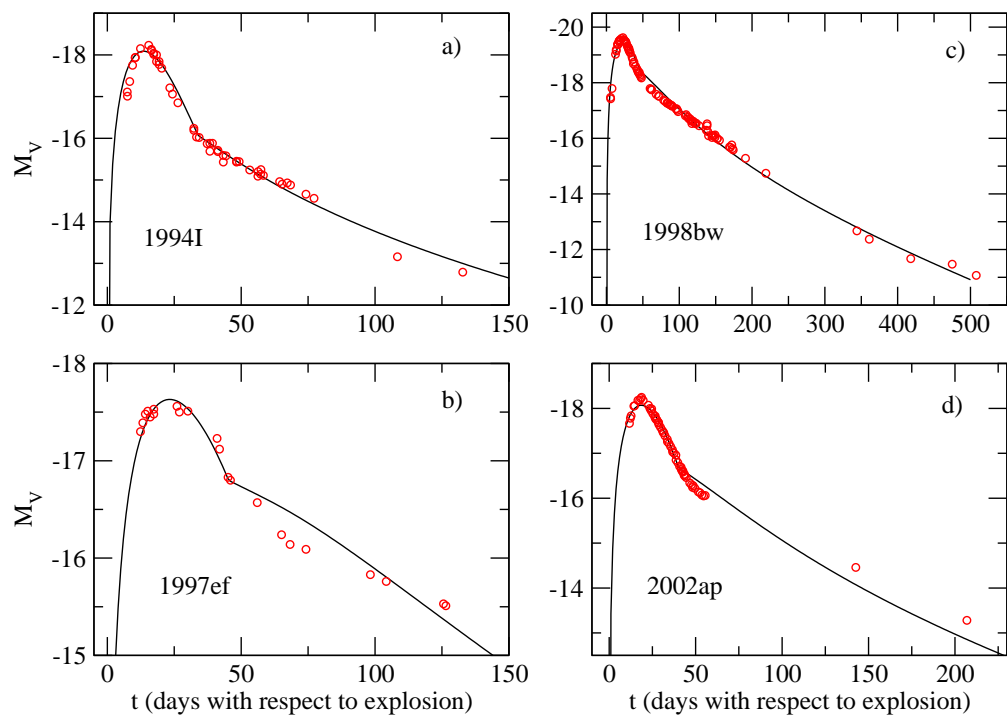


Fig. 14.— The best fit for more SNe Ic; b) – c) are hypernovae (graphs are scaled independently).

Table 1. Absolute–Magnitude Data for SNe IIb

SN	Galaxy	V	$\mu$	$A_V$ (Galactic)	$A_V$ (host)	$M_V$
1987K	NGC4651	$14.4 \pm 0.3(1)$	$31.09 \pm 0.03^a(2)$	$0.088 \pm 0.014$	$0.2 \pm 0.2(3)$	$-17.0 \pm 0.4$
1993J	NGC3031	$10.86 \pm 0.02(4)$	$27.80 \pm 0.08^a(5)$	$0.266 \pm 0.043$	$0.36 \pm 0.22(6)$	$-17.57 \pm 0.24$
1996cb	NGC4651	$13.90 \pm 0.03(7)$	$31.09 \pm 0.03^a(2)$	$0.100 \pm 0.016$	$0.10 \pm 0.10(7)$	$-17.39 \pm 0.11$

<sup>a</sup>Cepheid calibrated distance

<sup>b</sup>Nearby Galaxies Catalog (Tully 1988)

<sup>c</sup>*Luminosity Distance* ( $H_0=60$ ,  $\Omega_M=0.3$ ,  $\Omega_\Lambda=0.7$ ; references are for redshifts)

References. — (1) Filippenko (1988), (2) Average of Cepheid distances for NGC4321, NGC4535, NGC4548 and NGC4639 in the same group; Freedman et al. (2001), (3) Filippenko (1987), (4) van Driel et al. (1993), (5) Freedman et al. (2001), (6) Richmond et al. (1994), (7) Qiu et al. (1999)

Table 2. Absolute–Magnitude Data for SNe Ib

SN	Galaxy	V	$\mu$	$A_V$ (Galactic)	$A_V$ (host)	$M_V$
1954A	NGC4214	$9.3 \pm 0.2(1,2)$	$27.13 \pm 0.23(3)$	$0.072 \pm 0.012$	$0.05 \pm 0.05(4)$	$-17.95 \pm 0.31$
1983N	NGC5236	$11.3 \pm 0.2(5)$	$28.25 \pm 0.15^a(6)$	$0.228 \pm 0.037$	$0.37 \pm 0.37(5)$	$-17.55 \pm 0.45$
1984I	E323–G99	$15.98 \pm 0.20(7)$	$33.66 \pm 0.20^c(8)$	$0.344 \pm 0.055$	$0.05 \pm 0.05(9)$	$-18.07 \pm 0.29$
1984L	NGC 991	$13.8 \pm 0.2(10)$	$31.85 \pm 0.20^b$	$0.091 \pm 0.015$	$0.23 \pm 0.23(10)$	$-18.37 \pm 0.36$
1990I	NGC4650A	$15.3 \pm 0.10(11)$	$33.30 \pm 0.28(11)$	$0.374 \pm 0.060$	$0.13 \pm 0.13(11)$	$-18.50 \pm 0.33$
1991D	LEDA84044	$16.4 \pm 0.3(12)$	$36.67 \pm 0.05^c(13)$	$0.205 \pm 0.033$	$0.05 \pm 0.05(12)$	$-20.52 \pm 0.31$
1998dt	NGC 945	$17.42 \pm 0.5(14)$	$34.45 \pm 0.14^c(15)$	$0.085 \pm 0.014$	$0.35 \pm 0.35(4)$	$-17.46 \pm 0.63$
1999di	NGC 776	$17.91 \pm 0.8(14)$	$34.60 \pm 0.13^c(16)$	$0.322 \pm 0.052$	$0.67 \pm 0.67(4)$	$-17.68 \pm 1.05$
1999dn	NGC7714	$16.48 \pm 0.3(14)$	$33.37 \pm 0.23^c(16)$	$0.174 \pm 0.028$	$0.05 \pm 0.05(17)$	$-17.11 \pm 0.38$
1999ex	IC5179	$16.63 \pm 0.04(18)$	$33.80 \pm 0.19^c(8)$	$0.067 \pm 0.011$	$1.39 \pm 1.00(19)$	$-18.63 \pm 1.02$
2000H	IC 454	$17.30 \pm 0.03(20)$	$34.11 \pm 0.16^c(8)$	$0.760 \pm 0.122$	$0.60 \pm 0.60(4,21)$	$-18.17 \pm 0.63$

<sup>a</sup>Cepheid calibrated distance

<sup>b</sup>Nearby Galaxies Catalog (Tully 1988)

<sup>c</sup>*Luminosity Distance* ( $H_0=60$ ,  $\Omega_M=0.3$ ,  $\Omega_\Lambda=0.7$ ; references are for redshifts)

References. — (1) Schaefer (1996), (2) Leibundgut et al. (1991) and references therein, (3) Drozdovsky et al. (2002), (4) Calculated from the NaI D line, (5) Clocchiatti et al. (1996), (6) Thim et al. (2003), (7) Estimated from Leibundgut, Phillips, & Graham (1990), (8) NED, (9) Phillips & Graham (1984), (10) Wheeler & Levrealt (1985), (11) Elmhamdi et al. (2004), (12) Benetti et al. (2002) and references therein, (13) Maza & Ruiz (1989), (14) Estimated from Matheson et al. (2001), (15) Jha et al. (1998), (16) Asiago SN Catalog; Barbon et al. (1999), (<http://web.pd.astro.it/~supern/>), (17) Ayani et al. (1999), (18) Stritzinger et al. (2002), (19) Hamuy et al. (2002), (20) Krisciunas & Rest (2000), (21) Benetti et al. (2000)

Table 3. Absolute–Magnitude Data for SNe Ic

SN	Galaxy	V	$\mu$	$A_V$ (Galactic)	$A_V$ (host)	$M_V$
1962L	NGC1073	$13.13 \pm 0.10(1)$	$31.39 \pm 0.20^b$	$0.130 \pm 0.021$	$0.80 \pm 0.80(2)$	$-19.19 \pm 0.83$
1964L	NGC3938	$13.6 \pm 0.3(3)$	$31.72 \pm 0.14^a(4)$	$0.071 \pm 0.011$	$0.56 \pm 0.56(2)$	$-18.75 \pm 0.65$
1983I	NGC4051	$13.6 \pm 0.3(5)$	$31.72 \pm 0.14^a(4)$	$0.043 \pm 0.007$	$0.93 \pm 0.31(5)$	$-19.09 \pm 0.45$
1983V	NGC1365	$13.80 \pm 0.20(6)$	$31.27 \pm 0.05^a(7)$	$0.068 \pm 0.011$	$0.56 \pm 0.22(6)$	$-18.10 \pm 0.30$
1987M	NGC2715	$14.7 \pm 0.3(8)$	$32.03 \pm 0.23^b$	$0.085 \pm 0.014$	$1.4 \pm 0.6(9)$	$-18.82 \pm 0.71$
1990B	NGC4568	$15.75 \pm 0.20(10)$	$30.92 \pm 0.05^a(7)$	$0.108 \pm 0.017$	$2.63 \pm 1.00(10)$	$-17.91 \pm 1.02$
1991N	NGC3310	$13.9 \pm 0.3(11,12)$	$31.84 \pm 0.20^b$	$0.075 \pm 0.012$	$1.0 \pm 1.0(13)$	$-19.02 \pm 1.06$
1992ar	ANON	$19.54 \pm 0.34(14)$	$39.52 \pm 0.01^c(15)$	$0.048 \pm 0.008$	$0.25 \pm 0.25(16)$	$-20.28 \pm 0.42$
1994I	NGC5194	$12.91 \pm 0.02(17)$	$29.62 \pm 0.15(18)$	$0.115 \pm 0.018$	$1.4 \pm 0.5(19)$	$-18.22 \pm 0.52$
1997ef	UGC 4107	$16.47 \pm 0.10(20)$	$33.90 \pm 0.18^c(21)$	$0.141 \pm 0.022$	$0.05 \pm 0.05(20)$	$-17.62 \pm 0.21$
1998bw	E184–G82	$13.75 \pm 0.10(22)$	$33.13 \pm 0.26^c(21)$	$0.194 \pm 0.031$	$0.05 \pm 0.05(23)$	$-19.62 \pm 0.28$
1999cq	UGC11268	$16.1 \pm 0.6(24)$	$35.64 \pm 0.08^c(21)$	$0.180 \pm 0.029$	$0.39 \pm 0.39(24)$	$-20.11 \pm 0.72$
2002ap	NGC 628	$12.37 \pm 0.04(25)$	$30.41 \pm 0.20^b$	$0.161 \pm 0.026$	$0.03 \pm 0.03(26)$	$-18.23 \pm 0.21$

<sup>a</sup>Cepheid calibrated distance

<sup>b</sup>Nearby Galaxies Catalog (Tully 1988)

<sup>c</sup>*Luminosity Distance* ( $H_0=60$ ,  $\Omega_M=0.3$ ,  $\Omega_\Lambda=0.7$ ; references are for redshifts)

References. — (1) Schaefer (1995), (2) Estimated from Porter & Filippenko (1987), (3) Leibundgut et al. (1991) and references therein, (4) Same group as NGC3982; Saha et al. (2001), (5) Tsvetkov (1985), (6) Clocchiatti et al. (1997), (7) Freedman et al. (2001), (8) Filippenko, Porter, & Sargent (1990), (9) Nomoto, Filippenko, & Shigeyama (1990), (10) Clocchiatti et al. (2001), (11) Tsvetkov (1994), (12) Korth (1991a) (13) Grothues & Schmidt-Kaler (1991), (14) Clocchiatti et al. (2000), (15) Phillips & Humay (1992), (16) Estimated from Clocchiatti et al. (2000), (17) Richmond et al. (1996), (18) Feldmeier, Ciardullo, & Jacoby (1997), (19) Barth et al. (1996), (20) Estimated from Iwamoto et al. (2000), (21) NED, (22) Galama et al. (1998), (23) Nakamura et al. (2001), (24) Estimated from Matheson et al. (2000), (25) Gal–Yam et al. (2002) (data actually taken from <http://wise-obs.tau.ac.il/~avishay/local/2002ap/index.html>), (26) Klose, Guenther, & Woitas (2002)

Table 4. Mean Absolute Magnitudes for Various Data Sets

Data Set	Weighted		Unweighted		
	$\overline{M}_V$	$\sigma$	$\overline{M}_V$	$\sigma$	N
All SE	$-18.03 \pm 0.06$	0.89	$-18.40 \pm 0.18$	0.94	27
Bright SE	$-20.08 \pm 0.18$	0.46	$-20.13 \pm 0.19$	0.38	4
Normal SE	$-17.77 \pm 0.06$	0.49	$-18.10 \pm 0.13$	0.63	23
IIB only	$-17.40 \pm 0.10$	0.15	$-17.32 \pm 0.17$	0.29	3
Ib only	$-18.37 \pm 0.12$	1.05	$-18.18 \pm 0.27$	0.91	11
Ic only	$-18.51 \pm 0.10$	0.86	$-18.84 \pm 0.23$	0.83	13
Normal Ib	$-17.98 \pm 0.13$	0.46	$-17.95 \pm 0.16$	0.49	10
Bright Ic	$-19.85 \pm 0.22$	0.37	$-20.00 \pm 0.20$	0.34	3
Normal Ic	$-18.14 \pm 0.12$	0.48	$-18.49 \pm 0.17$	0.55	10

Table 5. Supernovae with Light Curves

SN Name	SN Type	Reference	SN Name	SN Type	Reference
1993J	IIb	(1),(2),(3)	1962L	Ic	(15)
1996cb	IIb	(4)	1983I	Ic	(16)
1954A	Ib	(5),(6),(7)	1983V	Ic	(17)
1983N	Ib	(8)	1987M	Ic	(18)
1984I	Ib	(9)	1990B	Ic	(19)
1984L	Ib	(10)	1991N	Ic	(20),(21),(22)
1990I	Ib	(11)	1992ar	Ic	(23)
1991D	Ib	(12)	1994I	Ic	(24),(25)
1999ex	Ib	(13)	1997ef	Ic	(26)
2000H	Ib	(14)	1998bw	Ic	(27),(28),(29)
			2002ap	Ic	(30),(31),(32)

References. — (1) Barbon et al. (1995), (2) van Driel et al. (1993), (3) Lewis et al. (1994), (4) Qiu et al. (1999), (5) Leibundgut et al. (1991), (6) Schaefer (1996), (7) Wellmann & Beyer (1955), (8) Clocchiatti et al. (1996), (9) Leibundgut, Phillips, & Graham (1990), (10) Baron, Young, & Branch (1993) and references therein, (11) Elmhamdi et al. (2004), (12) Benetti et al. (2002), (13) Stritzinger et al. (2002), (14) Krisciunas & Rest (2000), (15) Bertola (1964) (16) Tsvetkov (1985), (17) Clocchiatti et al. (1997), (18) Filippenko, Porter, & Sargent (1990), (19) Clocchiatti et al. (2001), (20) Korth (1991a), (21) Korth (1991b), (22) Tsvetkov (1994), (23) Clocchiatti et al. (2000), (24) Clocchiatti et al. (1997), (25) Richmond et al. (1996), (26) Iwamoto et al. (2000), (27) Galama et al. (1998), (28) McKenzie & Schaefer (1999), (29) Sollerman et al. (2000), (30) Foley et al. (2003), (31) Pandey et al. (2003), (32) Yoshii et al. (2003)

Table 6. Parameters of the Best Light-Curve Fits

SN name	$E_k$ (foe)	$M_{ej}$ ( $M_\odot$ )	$M_{Ni}$ ( $M_\odot$ )	$t_{rise}$ (days)	$\chi^2_r$	$\delta M_V$ (mag)	N
IIb							
1993J	0.66(1)	1.3	0.10	20	2.14	0.26	89
1996cb	0.22(2)	0.9	0.08	20	1.30	0.18	44
Ib							
1983N	0.30(3)	0.8	0.10	18	2.27E–2	0.45	9
1984L	2.16(2)	4.0	0.92	27	2.63	0.91	17
1984L pk	0.97(2)	1.8	0.37	22	0.144	0.91	17
1990I	0.67(2)	1.2	0.18	20	0.743	1.17	32
1991D	0.25(2)	1.9	$\geq 1.52$	27	4.42	0.49	10
1999ex	0.30(2)	0.9	0.25	19	0.967	1.05	71
Ic							
1962L	0.11(2)	0.6	0.37	19	6.92E–3	0.85	11
1983I	0.33(3)	0.7	0.23	17	0.140	0.46	18
1983V	0.99(2)	1.3	0.15	19	3.25E–3	0.35	5
1987M	0.19(4)	0.4	0.13	14	3.49E–3	0.72	4
1990B	0.55(2)	0.9	0.14	18	0.229	1.08	26
1992ar	1.14(2)	1.5	0.84	20	0.103	0.67	7
1994I	0.55(5)	0.5	0.08	14	0.744	0.53	50
1997ef	3.26(6)	3.1	0.16	23	0.491	0.23	22
1998bw	31.0(7)	6.2	0.78	23	2.26	0.41	105
2002ap	2.72(8)	1.7	0.14	19	1.50	0.23	60

References. — For  $E_k/M_{ej}$  relation – (1) Blinnikov et al. (1998), (2)  $E_k/M_{ej}$  was calculated as described in text, (3) Shigeyama et al. (1990), (4) Nomoto, Filippenko, & Shigeyama (1990), (5) Young, Baron, & Branch (1995), (6) Iwamoto et al. (2000), (7) Nakamura et al. (2001) (8) Mazzali et al. (2002)

Table 7. Results Compared to Other Studies

SN	Study	$E_k$ (foe)	$M_{ej}$ ( $M_\odot$ )	Comments
IIb				
1993J	This paper	0.66	1.3	
	This paper (impose $E_k = 1$ foe)	1	1.6	
	Young, Baron, & Branch (1995)	1	2.6	
	Blinnikov et al. (1998)	1.2	2.45	
Ib				
1983N	This paper	0.30	0.8	No $^{56}\text{Ni}$ mixing
	This paper (impose $E_k = 1$ foe)	1	1.3	No $^{56}\text{Ni}$ mixing
	Shigeyama et al. (1990)	1	2.7	Extensive $^{56}\text{Ni}$ mixing
1990I	This paper	0.67	1.2	
	This paper (impose $E_k = 1$ foe)	1	1.4	
	Elmhamdi et al. (2004)	1	3.7	late-times only
Ic				
1983I	This paper	0.33	0.7	No $^{56}\text{Ni}$ mixing
	This paper (impose $E_k = 1$ foe)	1	1.1	No $^{56}\text{Ni}$ mixing
	Shigeyama et al. (1990)	1	2.1	Extensive $^{56}\text{Ni}$ mixing
1987M	This paper	0.19	0.4	No $^{56}\text{Ni}$ mixing
	This paper (impose $E_k = 1$ foe)	1	0.8	No $^{56}\text{Ni}$ mixing
	Nomoto, Filippenko, & Shigeyama (1990)	1	2.1	Extensive $^{56}\text{Ni}$ mixing
1997ef	This paper	3.3	3.1	
	Iwamoto et al. (2000)	8	7.6	
1998bw	This paper	31	6.2	
	Nakamura et al. (2001)	50	10	
	Woosley, Eastman, & Schmidt (1999)	22	6.5	
2002ap	This paper	2.7	1.7	
	Mazzali et al. (2002)	4 – 10	2.5 – 5	